

Interference of Magnetic-Dipole and Electric-Dipole Interactions in Semiconductors

Yang-Fang Chen (陳永芳)

Physics Department, National Taiwan University

Taipei, Taiwan IO 764, R. O. C.

(Received Jan. 20, 1990)

We have shown that the anomalous dependence of spin-resonance intensity on the sign of either the dc magnetic field \vec{B}_0 or the wave vector \vec{q} of the photon observed in **InSb** can be understood by the interference between electric-dipole and magnetic-dipole interactions when the former become allowed by virtue of mixing of Landau and Zeeman levels by a spin-orbit interaction lacking inversion symmetry. A **theoretical** study of this phenomenon in semiconductors with zinc-blende structure is presented for the principle experimental configurations. This effect provides an elegant way to obtain the parameter which causes the **electric-dipole**-induced spin resonance. We also investigate the electric-dipole and magnetic-dipole interference in semi-conductor with **wurtzite** structure.

I. INTRODUCTION

Many interesting phenomena will appear when there are more than one interaction which can simultaneously produce the same transition. Even if one of the interaction is rather weaker than the other, the unexpected effects can still exist due to the interference between the interactions. Examples include optical activity in molecule¹ and magneto-electric effect² in magnetic crystal. In this paper we will concentrate the peculiar experimental observation of the conduction electron spin resonance in **InSb**.^{3,4} The unusual behavior of **InSb** magnetotransmission spectra at spin resonance (SR) observed on reversing applied dc magnetic field \vec{B}_0 or the wave vector \vec{q} of the photon is illustrated by the data shown in Fig. 1. Fig. 1(a) shows the SR signal for $\vec{B}_0 \parallel [110]$ (in the face of the sample), with $\vec{q} \parallel [1\bar{1}0]$ (normal to the sample). Fig. 1(b) shows SR when the sample is rotated by 180° about \vec{q} with respect to Fig. 1(a). Fig. 1(c) is for the sample rotated by 180° about \vec{B}_0 relative to Fig. 1(a) (i.e., flipped front to back about the $[110]$ axis), without changing the direction of \vec{q} in the laboratory frame. Fig. 1(d) is observed for the sample rotated by 180° about $\vec{q} \times \vec{B}_0$ relative to Fig. 1 (a) (in this case, flipped front to back about the $[001]$ cubic axis). Figs. 1 (a') - 1(d') show SR observed with the field reversed relative to Figs. 1 (a)-1 (d), respectively. The following features emerge from the figure.

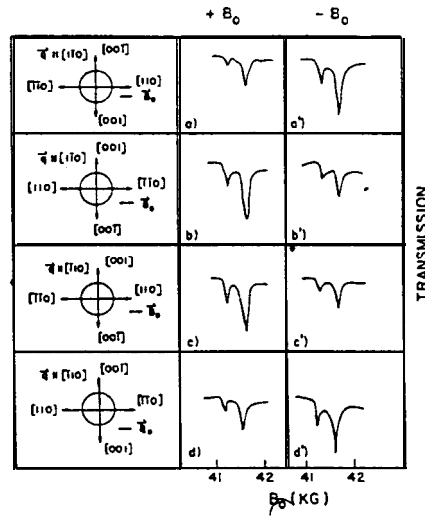


FIG. 1. Symmetry characteristics of spin resonance in InSb, observed at $118.8 \mu\text{m}$ and 4.5 K . (a) spin resonance for $\vec{B}_0 \parallel [1\bar{1}0]$, $\vec{q} \parallel [110]$; (b) the sample was rotated by 180° about \vec{q} relative to (a); (c) the sample was rotated by 180° about $\vec{q} \times \vec{B}_0$ relative to (a). The sequence (a')-(d') corresponds to configurations (a)-(d), respectively, but with the magnetic field reversed. In each resonance doublet the higher-field, stronger line is the conduction-electron spin resonance, and the weak line is spin resonance of donor-bound electrons.

- (1) The intensity of SR changes quite strongly (by a factor of about 2) when the direction of the magnetic field is reversed relative to the crystallographic directions. This is observed by reversing the field itself [compare, e.g., Figs. 1 (a) and 1 (a')] or by rotating the sample by 180° about \vec{q} while keeping \vec{B}_0 fixed in the laboratory frame [compare Fig. 1 (a) and 1 (b)].
- (2) It is easily shown that rotating the sample by 180° about \vec{B}_0 is equivalent to reversing the direction of \vec{q} relative to the crystallographic directions, while keeping \vec{B}_0 fixed relative to the crystal frame. A change in SR intensity similar to that which takes place on reversing \vec{B}_0 is observed when \vec{q} is reversed in this manner [compare Figs. 1 (a) and 1 (c)].
- (3) Rotating the sample about $\vec{q} \times \vec{B}_0$ is equivalent to reversing the direction of both \vec{q} and \vec{B}_0 with respect to the sample. This operation leaves the SR intensity unchanged [compare Fig. 1 (a) with Fig. 1 (d); Fig. 1(a') with Fig. 1 (d')].

We will demonstrate that this peculiar phenomena are due to the simultaneous excitation of spin resonance of electric dipole and magnetic dipole interactions. We further investigate the effects for semiconductors with wurtzite structure. In view of the recent observation of electric dipole spin resonance in $\text{Cd}_{1-x}\text{Mn}_x\text{Se}$,⁵ such analysis would be useful and timely.

II. GENERAL EXPRESSION FOR THE ELECTRIC DIPOLE AND MAGNETIC DIPOLE INTERFERENCE

When an electromagnetic wave with a vector potential A' acts on a charged particle, the perturbation Hamiltonian has the form

$$H' = \frac{e}{c} \mathbf{V} \cdot \mathbf{A}' + \frac{g\beta_0}{2} \boldsymbol{\sigma} \nabla \times \mathbf{a}' , \quad (1)$$

where V is the velocity operator, g is the g factor of the electron, $\beta_0 = e\hbar/2m_0 c$ is the Bohr magneton, m_0 is the mass of the free electron, $\boldsymbol{\sigma} = (\sigma_x, \sigma_y, \sigma_z)$ is the Pauli matrix, and A' is the vector potential of the electromagnetic wave,

$$\mathbf{A}' = \text{Re}(\mathbf{A}'_0 e^{i(\omega t - \mathbf{q} \cdot \mathbf{r})}) . \quad (2)$$

Our task is to solve the time-dependent Schrodinger equation

$$i\hbar \frac{\partial \psi}{\partial t} = (H_0 + H')\psi , \quad (3)$$

where H_0 is the unperturbed Hamiltonian, which is time independent. The eigenstates of the unperturbed system are given by

$$H_0 \phi_m = E_m \phi_m . \quad (4)$$

The solution for the wave function ψ may be written as

$$\psi = \sum_m a_m(t) \phi_m(\mathbf{r}) e^{-iE_m t/\hbar} = \sum_m a_m \phi_m e^{-iE_m t/\hbar} \quad (5)$$

Following elementary time-dependent perturbation theory, we obtain

$$a_m = \frac{1}{2\hbar} \frac{e}{c} \mathbf{V}_{mn} \cdot \mathbf{A}'_0 \left[\frac{1 - e^{i(\omega_{mn} + \omega)t}}{\omega_{mn} + \omega} + \frac{1 - e^{i(\omega_{mn} - \omega)t}}{\omega_{mn} - \omega} \right] - \frac{1}{2\hbar} \mathbf{M}_{mn} \cdot (\mathbf{q} \times \mathbf{A}'_0) \times \left[\frac{1 - e^{i(\omega_{mn} + \omega)t}}{\omega_{mn} + \omega} - \frac{1 - e^{i(\omega_{mn} - \omega)t}}{\omega_{mn} - \omega} \right] , \quad (6)$$

where V_{mn} and M_{mn} are matrix elements corresponding to the electric- and magnetic-dipole terms, respectively, given by

$$V_{mn} = \int \phi_m^* \mathbf{V} \phi_n \, d\mathbf{r} \equiv \langle m | \mathbf{V} | n \rangle , \quad (7)$$

$$M_{mn} = \int \phi_m^* \mathbf{M} \phi_n \, d\mathbf{r} \equiv \langle m | \mathbf{M} | n \rangle , \quad (8)$$

$M = g\beta_0 \sigma/2$ is the magnetic-dipole moment, and

$$\omega_{mn} = \frac{E_m - E_n}{\hbar} \quad (9)$$

In Eq. (6) we have neglected the retardation factor by assuming that A' varies slowly in space. For the case of resonance, only terms which have the difference $\omega_{mn} - \omega$ in the denominator are important. The transition probability per unit time from the initial state $|n\rangle$ to a particular excited state $|m\rangle$ is then given by

$$W = \frac{\pi}{2\hbar^2} \left| \frac{e}{c} V_{n'n} \cdot A'_0 + iM_{n'n} \cdot (\mathbf{q} \times A'_0) \right|^2 \delta(\omega - (\omega_{n'} - \omega_n)) , \quad (10)$$

where energy-broadening effects have been neglected. The corresponding absorption coefficient α , with the occupation factors for initial and final states included, then becomes

$$\alpha = \frac{4\pi^2 c}{\Omega n \omega \hbar} \left| \frac{e}{c} V_{n'n} \cdot \hat{\xi} + iM_{n'n} \cdot (\mathbf{q} \times \hat{\xi}) \right|^2 \times (f_n - f_{n'}) \delta(\omega - (\omega_{n'} - \omega_n)) , \quad (11)$$

where Ω is the volume of the crystal, n is the refractive index, $\hat{\xi}$ is the polarization unit vector, and f_n is the probability that state n is occupied. Expanding the above equation, we obtain

$$\alpha = \frac{4\pi^2 c}{\Omega n \omega \hbar} \left[\left| \frac{e}{c} V_{n'n} \cdot \hat{\xi} \right|^2 - 2\text{Re} \left[i \frac{e}{c} (\hat{\xi} \cdot V_{n'n}) [M_{n'n} \cdot (\mathbf{q} \times \hat{\xi})]^* \right] + \left| iM_{n'n} \cdot (\mathbf{q} \times \hat{\xi}) \right|^2 \right] (f_n - f_{n'}) \delta(\omega - (\omega_{n'} - \omega_n)) . \quad (12)$$

In addition to the usual absorption coefficient associated with the square of the matrix element of the electric-dipole transition, Eq. (12) contains a magnetic-dipole contribution, as well as an electric- and magnetic-dipole (EDMD) interference term. From the above equation we can see immediately that reversing the direction of propagation (which changes the sign of the wave vector \mathbf{q}) results in changing the sign of the interference term. It will also be shown later that reversing the direction of \mathbf{B}_0 changes the sign of $V_{n'n}$, which has a similar effect on the interference term. Thus, because of the electric-dipole and magnetic-dipole interference, the absorption spectrum can now depend on the sign of either \mathbf{B}_0 or \mathbf{q} .

III. ELECTRIC DIPOLE AND MAGNETIC DIPOLE INTERFERENCE IN ZINC-BLENDE SEMICONDUCTORS

We now turn to the analysis of the electric dipole and magnetic dipole (EDMD) interference at the conduction-electron-spin-resonance condition in zinc-blende semiconductors, with particular attention given to the dependence of the effect on the sign of \mathbf{B}_0 and \mathbf{q} , and

on the orientation of \mathbf{B}_0 and \mathbf{q} relative to the crystallographic axes. The precise nature of the effects of EDMD interference-which arises from the coupling between the electric-dipole and the magnetic-dipole terms in the Hamiltonian, depends upon band-structure details of the particular material considered. For zinc-blende semiconductors the EDSR can arise from three possible sources: the lack of inversion symmetry,^{6,7} wave-function mixing through $\mathbf{k}\cdot\mathbf{p}$ interaction⁸ (non-parabolicity), and/or warping.⁷ As shown by Chen et al,⁴ we know from experimental data that EDSR in InSb is dominated by inversion asymmetry, and we will therefore confine our analysis to that mechanism.

We use an effective-mass Hamiltonian in a magnetic field, generalized to include the term contributed by inversion asymmetry and the magnetic-dipole term. In the analysis of the anisotropy of the effect, we essentially follow the formalism developed by Rashba and Sheka,⁵ but we retain the magnetic-dipole matrix element along with the electric-dipole term throughout the analysis. Retaining terms up to third order in \mathbf{k} , the effective-mass Hamiltonian is given by⁹

$$H = \frac{\hbar^2 \mathbf{k}^2}{2m^*} + \frac{g\beta_0 \boldsymbol{\sigma} \cdot \mathbf{B}_0}{2} + \delta_0 \boldsymbol{\sigma} \cdot \boldsymbol{\kappa} \quad (13)$$

where m^* is the effective mass, $\hbar\mathbf{k}$ is the kinematic momentum associated with the vector potential \mathbf{A} of the dc magnetic field,

$$\hbar\mathbf{k} = -i\hbar\nabla + \frac{e}{c}\mathbf{A} \quad , \quad (14)$$

δ_0 is a parameter which is associated with spinorbital interaction and the inversion asymmetry, and $\boldsymbol{\kappa}$ is a vector given by

$$\kappa_x = k_y k_x k_y - k_z k_x k_z \quad , \quad (15)$$

with the indices x , y , and z corresponding to the cubic crystal axes. κ_y and κ_z are obtained from κ_x by cyclical permutation of the indices.

As shown in Ref. 6, when the inversion asymmetry contribution in the Hamiltonian is treated as a perturbation, the matrix elements of electric-dipole spin-flip transitions have the form

$$\begin{aligned} E_d &= \frac{e}{c} \sum_{\alpha} \langle l, - | V_{\alpha} | l, + \rangle \\ &= \sqrt{2} \frac{\delta_0 e^2 B_0}{c^2 \hbar^2} \sum_{\alpha} \frac{-\beta_{\alpha}}{q_{\alpha} - \beta^*} B_{(\alpha 12)} (2l + 1 - 2\xi^2) \quad , \end{aligned} \quad (16)$$

for an arbitrary magnetic field orientation and arbitrary polarization. Here l is the Landau-level quantum number of the initial and final states; $\alpha = 1, 2, 3$, is the polarization index corresponding to left-circular [cyclotron-resonance-active (CRA)] , right-circular [cyclotron-resonance-inactive (CRI)] , and parallel Voigt ($\mathbf{E} \parallel \mathbf{B}_0$) polarizations, respectively; and q_{α} is

the change in Landau quantum number under the action of the operator a_α , where

$$a_- = \left[\frac{c\hbar}{2eB_0} \right]^{1/2} (k_x - ik_y)$$

$$a_+ = \left[\frac{c\hbar}{2eB_0} \right]^{1/2} (k_x + ik_y),$$

$$a_z = \left[\frac{c\hbar}{eB_0} \right]^{1/2} k_z \equiv \xi$$

(i.e., a_- and a_+ are lowering and raising operators, respectively, for inter-Landau-level transitions). Thus $q_\alpha = -1, 1$ or 0 as $a = 1, 2$, or 3 , respectively. Further, $\beta^* = m^*g/2m_0$ is the ratio of the spin splitting to the cyclotron spacing, and $B_{(\alpha 12)}$ are trigonometric functions of the angle between the crystal axes and B_0 , derived in Ref. 5. These functions—which contain all information concerning the anisotropy of the matrix element for electric dipole transitions—are as follows:

$$\begin{aligned} B_{(112)} &= -\frac{1}{2} \cos(2\phi) \cos(2\theta) + \frac{1}{4} \sin(2\phi) \cos\theta (2 \cos^2\theta - \sin^2\theta), \\ B_{(212)} &= \frac{3i}{4} \sin(2\phi) \sin\theta \sin(2\theta), \\ B_{(312)} &= \frac{-3i}{4\sqrt{2}} [\cos(2\phi) \sin(2\theta) - i \sin(2\phi) \sin\theta (2 \cos^2\theta - \sin^2\theta)], \end{aligned} \quad (17)$$

where θ and ϕ are the polar and azimuthal angle of the magnetic field B_0 , respectively. Note that the matrix element of V_α in Eq. (16) is linear in B_0 ; i.e., it changes sign when the direction of B_0 is reversed, as has already been mentioned.

Proceeding similarly as in the calculation for the electric-dipole transition, we obtain the matrix element for the magnetic-dipole term,

$$\begin{aligned} M_d &= \frac{1}{2} g\beta_0 \langle l, - | \delta_\alpha | l, + \rangle (q \times \hat{\xi})_\alpha \\ &= \frac{i\sqrt{2}}{2} g\beta_0 (q \times \hat{\xi})_\alpha \delta_{\alpha 2} \end{aligned} \quad (18)$$

In this expression M_d (which depends on the components of the magnetic field of the incident wave expressed in the coordinate system where $\hat{z} \parallel B_0$) is not necessarily isotropic, and may contain both real and imaginary parts. This feature is a consequence of the particular choice of coordinates. However, the resonance intensity, which is proportional to $|M_d|^2$, is isotropic—i.e., independent of θ and ϕ —for all the principal geometries, as would be expected. We will examine these properties in a later section.

Substituting Eqs. (16) and (18) into Eq. (12), we obtain the absorption coefficient for the spin resonance, including the EDMD interference terms, for zinc-blende crystal:

$$\begin{aligned}
 \alpha &= \frac{8\pi cN}{n\omega\hbar\gamma} \left[\left| \sqrt{2} \frac{\delta_0 e^2 B_0}{c^2 \hbar^2} \frac{-\beta^*}{q_\alpha - \beta^*} B_{(\alpha 12)} \right|^2 \right. \\
 &\quad + 2\text{Re} \left[\frac{i\delta_0 e^2 B_0}{\hbar^2 C^2} \frac{-\beta^*}{q_\alpha - \beta^*} g\beta_0 B_{(\alpha 12)} g\beta_0 B_{(\alpha 12)} (\mathbf{q} \times \hat{\xi})_2^* \right] \\
 &\quad \left. + \left| \frac{i\sqrt{2}}{2} g\beta_0 (\mathbf{q} \times \hat{\xi})_2 \right|^2 \right] \\
 &= \frac{8ncN}{n\omega\hbar\gamma} \left[\left| E_d \right|^2 + 2\text{Re}(E_d M_d^*) + \left| M_d \right|^2 \right]. \tag{19}
 \end{aligned}$$

In Eq. (19) we have assumed that the broadening parameter γ is the same for the electric- and the magnetic-dipole transitions. This assumption is physically justified because the above formulation is for a single electron undergoing the same transition (and therefore experiencing the same level broadening) under the simultaneous action of an electric and a magnetic field. We have neglected the small contribution of \mathbf{k}_z , and the N in the equation is the carrier concentration. Using Eq. (19), we shall now examine the EDMD interference in the principal experimental configurations.

III-1 Faraday Geometry

The Faraday geometry refers to the configuration where wave propagation is parallel to the dc magnetic field. In this case there are two normal modes which can be supported by the medium, the cyclotron-resonance-active (CRA) polarization, i.e., that circular polarization which excites cyclotron resonance of conduction electrons, and the cyclotron-resonance-inactive (CRI) polarization. For the CRA polarization there is no magnetic-dipole transition because $g < 0$, and the EDMD interference will therefore vanish for this mode. In the CRI polarization, the matrix element for the electric-dipole transition at sufficiently low electron concentrations and high magnetic fields (so that only the ground state is occupied) is

$$\begin{aligned}
 E_d &= \sqrt{2} \frac{\delta_0 e^2 B_0}{\hbar^2 c^2} \frac{\beta^*}{\beta^* - 1} B_{(212)} \\
 &= \frac{i3\sqrt{2}}{4} \frac{\delta_0 e^2 B_0}{\hbar^2 c^2} \frac{\beta^*}{\beta^* - 1} \sin(2\phi) \sin\theta \sin(2\theta). \tag{20}
 \end{aligned}$$

From Eq. (18), the matrix element for the magnetic-dipole transition for CRI excitation is

$$M_d = \frac{\sqrt{2}}{2} g\beta_0 q, \tag{21}$$

where $q = \omega n/c$ is the wave vector inside the medium, n being the index of refraction. We immediately see that for this polarization M_d and E_d are always out of phase (one is

imaginary while the other one is real), and the interference again vanishes.

We thus conclude that there is no EDMD interference at spin resonance in the Faraday geometry, and consequently the spectrum does not depend on the sign of \mathbf{B}_0 or q . (Note that \mathbf{B}_0 reversal of course changes CRA to CRI in the Faraday geometry. What we mean here is that there is no change in the spin-resonance intensity when \mathbf{B}_0 and the circular polarization are reversed simultaneously, or when the sample is flipped front to back.)

III-2 Voigt Geometry

The configuration where the propagation of the wave is perpendicular to the dc magnetic field is referred to as the Voigt geometry. There are two independent modes which can be supported by the medium in this geometry: the parallel, or ordinary Voigt geometry (OV), where the electric field is parallel to the dc magnetic field (and the magnetic field \mathbf{H}' of the wave is perpendicular to \mathbf{B}_0); and the perpendicular, or extraordinary Voigt geometry (EV), where the electric field is perpendicular to \mathbf{B}_0 , and the magnetic field of the wave is parallel to \mathbf{B}_0 .

We see immediately that the EV geometry does not manifest magnetic-dipole spin resonance because there $\mathbf{H}' \parallel \mathbf{B}_0$, so that $\mathbf{M}_d = 0$, and hence the interference also disappears. The OV geometry, on the other hand, turns out to be most interesting in the spin-resonance context, and we will investigate it in detail. In particular, we shall examine the angular dependence of spin resonance in this geometry for the dc magnetic field in different planes. Here we only show the case of $\vec{\mathbf{B}}_0$ in the (112) plane.

From Eqs. (16) and (17), the matrix element for the EDSR transition in the OV geometry, for the magnetic field in an arbitrary plane, is given by

$$\begin{aligned} E_d &= \sqrt{2} \frac{\delta_0 e^2 B_0}{\hbar^2 c^2} B_{(312)} \\ &= -\frac{3}{4} \frac{\delta_0 e^2 B_0}{\hbar^2 c^2} \cos(2\phi) \sin(2\theta) - i \sin(2\phi) \sin\theta (2 \cos^2\theta - \sin^2\theta) \end{aligned}$$

For $\vec{\mathbf{B}}_0$ in the (112) plane \mathbf{M}_d is given by

$$\mathbf{M}_d = i \frac{g\beta_0}{2} q \frac{1}{\sqrt{6}} [\cos\theta (\sin\phi - \cos\phi) + 2\sin\theta + i(\sin\phi + \cos\phi)] \quad (23)$$

Here, ϕ and θ have to satisfy the following constraints:

$$\cos\theta = \frac{1}{\sqrt{3}} \sin\beta \quad (24)$$

$$\tan\phi = \frac{\sqrt{3} \cos\beta + \sqrt{2} \sin\beta}{\sqrt{3} \cos\beta - \sqrt{2} \sin\beta}, \quad (25)$$

where β is the angles between the [110] direction and $\vec{\mathbf{B}}_0$. Thus, the \mathbf{M}_d and E_d matrix elements both contain real and imaginary parts. There will have interference between the

in-phase terms. The total absorption coefficient for the spin resonance are given below:

$$\begin{aligned} \alpha = & \frac{8\pi c N}{n\omega \hbar \gamma} \left[\left[\frac{3\delta_0 e^2 B_0^2}{4c^2 \hbar^2} \{ [\cos(2\phi) \sin(2\phi)]^2 + [\sin(2\phi) \sin\theta (2\cos^2\theta - \sin^2\theta)]^2 \} \right. \right. \\ & + \frac{3}{4} - \frac{\delta_0 e^2 B_0}{c^2 \hbar^2} g\beta_0 q \{ \cos(2\phi) \sin(2\theta) [\cos\theta (-\sin\phi + \cos\phi) - 2\sin\theta] \\ & \left. \left. + \sin(2\phi) \sin\theta (2\cos^2\theta - \sin^2\theta) (\cos\phi + \sin\phi) + \left[\frac{g\beta_0 q}{2} \right]^2 \right] \right] \end{aligned}$$

In Eqs. (26) the first term represents the absorption coefficient for "bare" EDSR, the second term is the contribution of the EDMD interference, and the third term gives the isotropic magnetic-dipole spin-resonance absorption.

Figure 2. shows the spin resonance absorption coefficient as a function of orientation of \vec{B}_0 in (112) plane. The measurements were performed on InSb at 118.8 μm and 4.5 K⁴.

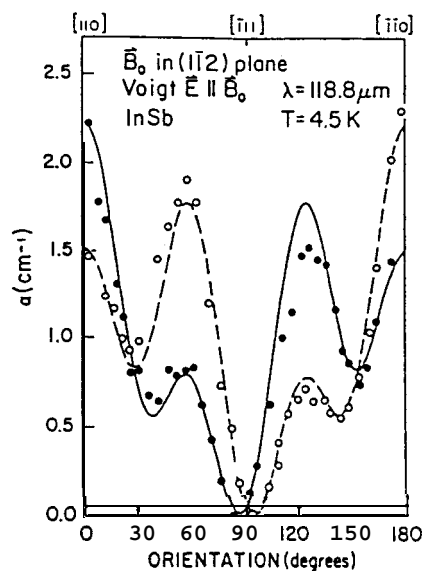


FIG. 2. Spin-resonance absorption coefficient of conduction electrons in InSb as a function of \vec{B}_0 in the (112) plane. Solid and open circles correspond to opposite signs of \vec{B}_0 , respectively. The solid and dashed curved are the theoretical angular dependences fitted to the experimental data for opposite field directions. The data were taken at 118.8 μm and 4.5 K.

Note the strong angular dependence of the data, and the absorption coefficients corresponding to opposite field directions, indicated by solid and open circles, respectively. The theoretical curves are obtained by adjusting the value of δ_0 , with the solid and dashed curves drawn for opposite directions of \vec{B}_0 . The agreement between experimental and theoretical angular dependence of the spin-resonance absorption coefficient provides an excellent demonstration of the existence of EDMD interference in zinc-blende semiconductors.

The interference provides a direct method for obtaining the parameters associated with inversion asymmetry. The obtained value is $\delta_0 = 56 \text{ a.u.}$ (atomic unit) or $3.6 \times 10^{-34} \text{ erg cm}^3$. Rashba and Sheka⁶ have estimated the value of δ_0 to be the order of 200 a.u. , but they point out that this estimate may differ significantly from the true value. Also Sugihara¹⁰ estimated δ_0 to be 100 a.u. by fitting the linewidth of microwave spin resonance data. We believe that the value of δ_0 obtained in our measurements is the best determination of this parameter to date.

IV. EDMD INTERFERENCE IN WURTZITE STRUCTURE

In this section we will investigate the EDMD interference in wurtzite semiconductors. The analysis is similar to that of the zinc-blende structure. The energy of carriers in a wurtzite crystal near the conduction band minimum has the form

$$H = \frac{\hbar^2 \mathbf{k}^2}{2m^*} + \frac{g\beta_0 \vec{\sigma} \cdot \vec{B}_0}{2} + \lambda \hat{c} \cdot (\vec{\sigma} \times \vec{k}), \quad (27)$$

where λ is the spinorbit interaction constant, c is the unit vector along hexagonal axis of the crystal. The last term shows the admixture of orbital and spin states of electrons in the field \vec{B}_0 caused by the spin-orbit interaction. It gives rise to spin-flip transitions within the electric dipole approximation. Thus, the simultaneous existence of electric dipole and magnetic dipole transitions makes the interference between them possible. The velocity operator \vec{V} in Eq. (1) now becomes

$$\vec{V} = \frac{\hbar \vec{k}}{m^*} + \frac{v\lambda}{\hbar} [\hat{c} \cdot (\vec{\sigma} \times \vec{k}), \vec{r}] \quad (28)$$

In order to proceed the calculation of transition matrix elements, it is convenient to perform a canonic transformation to all the operators

$$A \rightarrow e^{\lambda T} A e^{-\lambda T}, \quad (29)$$

such that the eigenstates of the transformed Hamiltonian H coincides with that of the Hamiltonian H_0 . This can be accomplished if

$$(\lambda \hat{c} \cdot (\vec{\sigma} \times \vec{k}) + [\lambda T, H_0])_{\text{nondiag.}} = 0 \quad (30)$$

where the matrix elements of T are equal to

$$\begin{aligned} \langle n' | T | n \rangle &= \frac{\langle n' | \hat{c} \cdot (\vec{\sigma} \times \vec{k}) | n \rangle}{E'_n - E_n}, \quad n' \neq n \\ &= 0, \quad n' = n \end{aligned} \quad (31)$$

The velocity operator in the new representation is given by

$$\vec{V} = \frac{\hbar \vec{k}}{m^*} + \frac{i\lambda}{\hbar} [\hat{c} \cdot (\vec{\sigma} \times \vec{k}), r] + \frac{\hbar}{m^*} [T, \vec{k}] \quad (32)$$

Using the same procedures as in Ref. 6, we obtain the transition matrix element of the electric dipole

$$E_d = \sum_{\alpha} \sqrt{2} \frac{e\lambda}{c\hbar} (B_{2\alpha} B_{21}^{-1} - B_{1\alpha} B_{22}^{-1}) \left(\frac{\beta^*}{\beta - q_{\alpha}} \right) \quad , \quad (33)$$

where B_{ij} is the matrix element of the transformation matrix B,

$$B = \begin{pmatrix} -\frac{1}{\sqrt{2}}(\sin\phi + i \cos\theta \cos\phi) & -\frac{1}{\sqrt{2}}(\sin\phi - i \cos\theta \cos\phi) \sin\theta \cos\phi & \\ \frac{1}{\sqrt{2}}(\cos\phi - i \cos\theta \sin\phi) & \frac{1}{\sqrt{2}}(\cos\phi + i \cos\theta \sin\phi) & \sin\theta \sin\phi \\ \frac{i}{\sqrt{2}}\sin\theta & -\frac{1}{\sqrt{2}}\sin\theta \cos\theta & \cos\theta \end{pmatrix}$$

and B_{ij}^{-1} is the matrix element of the matrix B^{-1} . The magnetic-dipole transition matrix element M_d is the same as in Eq. (18). Thus, using Eq. (33) and (18) we can examine the EDMD interference in the principal experimental configurations.

IV-1 Faraday Geometry

Since there is no magnetic dipole resonance in CRA geometry, EDMD interference does not exist in this configuration. For CRI geometry,

$$E_d = \sqrt{2}i \frac{e\lambda}{c\hbar} \cos\theta \quad , \quad (34)$$

$$M_d = \frac{g\beta_0 q}{2} \quad . \quad (35)$$

Thus, E_d and M_d are out of phase, and hence the interference is also disappear.

IV-2 Voigt Geometry

In the parallel Voigt geometry,

$$E_d = \frac{e\lambda}{c\hbar} \sin\theta \quad . \quad (36)$$

It \vec{B}_0 is in the plane perpendicular to \hat{c} axis, we have

$$M_d = \frac{1}{2} g\beta_0 q (\cos\phi)^2 \quad (37)$$

Comparing Eqs. (36) and (37), we note that both matrix elements are real, and EDMD interference will therefore occur. The total absorption coefficient is then given by

$$\alpha = \frac{8\pi cN}{n\omega\hbar r} \left[\left(\frac{e\lambda}{c\hbar} \sin\theta^2 \right) + \frac{1}{2} \frac{e\lambda}{c\hbar} g\beta_0 q \sin\theta (\cos\phi)^2 + \left(\frac{1}{2} g\beta_0 q (\cos\phi)^2 \right)^2 \right] \quad (38)$$

Thus, unlike the spin resonance in zinc-blende semiconductors which has the intensity depending on the sign of \vec{B}_0 or \vec{q} , the spin resonance in wurtzite semiconductors depends only on the sign of the wave vector of the photon. Since the electric-dipole spin resonance has been observed in wurtzite **semiconductors**, we believe the interference effect described here is readily investigated. The spinorbit interaction constant should be able to be determined accurately.

V. SUMMARY AND FUTURE WORK

This work demonstrates that the anomalous dependence of spin-resonance intensity on the sign of either the dc magnetic field \vec{B}_0 or the wave vector \vec{q} of the photon observed in **InSb** can be understood by the interference between electric-dipole and magnetic-dipole interactions. Using the effective-mass approximation, a theoretical study of this phenomena in zinc-blende semiconductors is developed. The results can be used to determine the inversion asymmetry parameter characterizing the spin-orbit interaction. It is believed that the value of this parameter obtained in our analysis is the best determination to date. We have extended this analysis to the electric-dipole and magnetic-dipole interference in semiconductors with wurtzite structure. Unlike the spin resonance in zinc-blende semiconductors, we found that the spin resonance in wurtzite semiconductors depends only on the sign of the wave vector of the photon. In view of the recent observation of **electric-dipole-spin-resonance** in $\text{Cd}_{1-x}\text{Mn}_x\text{Se}$,⁵ the interference effect described here is readily investigated, and hence the spin-orbit interaction constant can be determined accurately. Furthermore, it is also very interesting to see the existence of the interference in other important semiconductors, such as **HgTe**, **HgCdTe**, and **GaAs** etc. Finally, we like to emphasize a very important point of the situation where more than one interaction can simultaneously produce the same transition. Even if one of the interaction is rather weaker than the others, the unexpected effects can still exist due to the interference between the interactions. Thus, the influence of the weaker interaction can not be ignored. For example, the transition probability of the magnetic-dipole interaction in **InSb** is about 2% of that of the electric-dipole interaction, but through the interference the magnetic-dipole transition can change the spin resonance intensity by a factor of two. We believe that the idea presented here may be able to be applied to the other branches of physics, and can resolve many peculiar phenomena.

ACKNOWLEDGMENTS

We like to thank Prof. J. K. Furdyna and Dr. M. Dobrowolska for valuable discussions.

This work was partially supported by the National Science Council of the Republic of China.

REFERENCES

1. E. U. Condon. *Rev. Mod. Phys.* 9,432 (1937).
2. T. H. O' Dell, *The Electrodynamics of Magnetolectric Media*, edited by E. P. Wohlfarth (North-Holland, Amsterdam, 1970).
3. M. Dobrowolska, Y. F. Chen, J. K. Furdyna, and S. Rodriguex, *Phys. Rev. Lett.* 51, 134 (1983).
4. Y. F. Chen, M. Dobrowolska, J. K. Furdyna, and S. Rodriguex, *Phys. Rev.* B32, 890 (1985).
5. M. Dobrowolska, A. Witowski, J. K. Furdyna, T. Ichiguchi, H. D. Drew, and P. A. Wolff, *Phys. Rev. Lett.* 49,845 (1982); *Phys. Rev.* B29, 6652 (1984).
6. E. I. Rashba and V. I. Sheka, *Fiz. Tver. Tela* 3, 1735 (1961); 3, 1863 (1961) [*Sov. Phys. - Solid State* 3, 1257 (1961); 3, 7357(1961)].
7. M. H. Weiler, R. L. Aggarwal, and B. Lax, *Phys. Rev.* B17, 3269 (1978).
8. Y. Yafet, in *Solid State Physics*, edited by F. Seitz and D. Turnbull (Academic, New York, 1963), 14, p. 1.
9. N. R. Ogg, *Proc. Phys. Soc.* 89, 43 1 (1966).
10. K. Sugihara, *J. Phys. Soc. Jpn.* 38, 1061 (1975).